Searching for Supersymmetry with the α_T variable in $p\bar{p}$ collisions with the CMS Detector at the Large Hadron Collider

Zoe Hatherell

A thesis submitted in fulfilment of the requirements
for the degree of Doctor of Philosophy
to Imperial College London
December 2011

Chapter 1

Searching for Supersymmetry with α_T in all-hadronic events

The analysis presented here represents a model-independent search for new physics in the all-hadronic channel. Designed to search for signs of supersymmetry whilst remaining sensitive to other new physics models, the strategy centers around a selection of events which fit a topology of heavy new particles pair-produced in p-p collisions, which decay through a chain with an end product which is stable and undetectable. This is achieved in the detector by identifying several jets with a large quantity of missing energy.

1.1 Monte-Carlo Samples

1.2 Trigger

In order to select the signal events and minimise the contamination from backgrounds, a set of selection criteria is applied. As described previously in Section TRIGG, data collected by the CMS detector is stored and organised according to the L1 and HLT trigger paths passed. Each given dataset then undergoes the offline event reconstruction described in Chapter RECON/IDEN, after which n-tuples are constructed from which we apply cuts on objects and analysis variables.

Previous incarnations of this analysis for the 2010 dataset REFF used a set of pure $H_T$triggers, however these are unsuitable for the 2011 analysis as these

have too high thresholds for the analysis due to the increase in instantaneous luminosity. The use of cross-object triggers is now employed, requiring events that pass thresholds in both $H_T$and $\not{H}_{\mathrm{T}}$ for the signal region, and using the lowest un-prescaled thresholds available to ensure signal yields are accurate. As this analysis makes use of those events which fail the selection criteria also, the hadronic control sample, the pre-scaled $H_T$triggers are still used taking into account the pre-scaled factors. In the muon control sample, due to the low p_{T}threshold we use the same triggers as for the hadronic signal sample, and the photon sample makes use of the single photon trigger paths.

Having passed one of the un-prescaled triggers the events are subjected to a series of cuts on objects and analysis variables in order to select the event topologies required and minimise the background contamination.

1.2.1 Pre-Selection

The events selected must be identified as good events from the CMS detector, using a pre-selection. It is required that events have at least one good primary vertex that is not fake, with N_{dof} ¿ 4 and a vertex position along he beam axis of —z_{vtx}— $<$ 24 cm and perpendicular to the axis of ρ ¡ 2 cm. Events that have many fake tracks are identified as monester events and removed, by requiring that the ratio of High Purity tracks to the total number be greater than 25% in events with more than 9 tracks.

Events where noise has been identified in the HCAL are removed also, using an algorithm which checks for Photodetectors which have at east 17 out of 18 channels with an E ¿ 1.5 GeV.

Events are then selected according to the following preselection:

- Require events with $\mathrm{N}_{jet} \geq 2$
- N_{muon}, $\mathrm{N}_{electron}$, $\mathrm{N}_{photon} = 0$ where $p_{\mathrm{T}\mu,e} \geq 10$ GeV, $p_{\mathrm{T}\gamma} \geq 25$ GeV
- $H_T \geq$ 275 GeV
- To protect the quantity α_{T} from the scenario where many jets exist below the momentum acceptance threshold, the missing energy variable $\not{H}_{\mathrm{T}}$ estimated from jet measurment is compared to the quantity $\not{E}_{\mathrm{T}}$ measured

from the calorimters. If the ratio $R_{miss} = \not{H}_T / \not{E}_T > 1.25$, the event is rejected.

1.2.2 Object Requirements and Vetoes

Jets

Muons

Electrons

Photons

CutFlow

1.2.3 Trigger

1.3 Data to Monte-Carlo Comparisons

1.3.1 Dependence of R_{α_T} on H_T

1.4 Data-Driven Background Estimation

1.4.1 Total background prediction

1.4.2 Estimating EWK background using high p_T using W+Jets events

Types of decay contributing to Muon Control Sample

1.4.3 Estimation Z $\nu\bar{\nu}$ + jets background using photon + jets events

1.5 Systematic Uncertainties

1.6 Simultaneous Fit

1.7 Limits

1.8 Conclusion

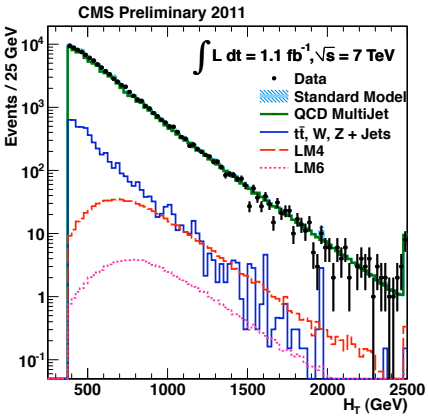

(a) Comparison of H_T between data and MC for the hadronic selection for $H_T \geq 375$ GeV and MHT > 100 GeV.

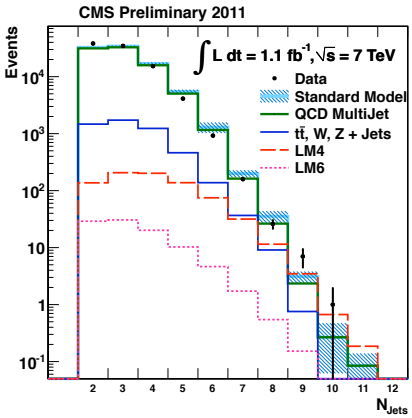

(b) Comparison of the jet multiplicity between data and MC for the hadronic selection, for $H_T \geq 375$ GeV and MHT > 100 GeV.

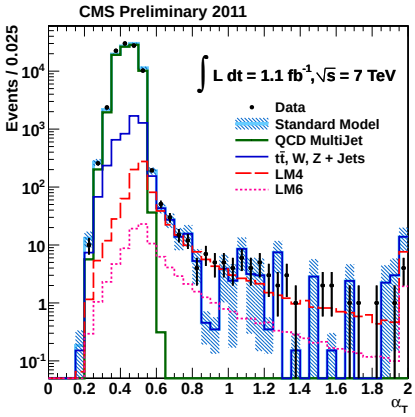

(c) Comparison of the α_T distribution between data and MC for the hadronic selection, for $H_T \geq 375$ GeV and MHT > 100 GeV.

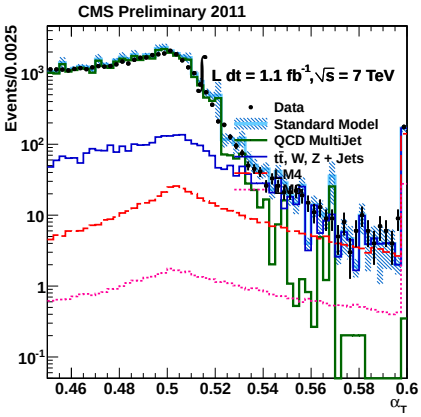

(d) Comparison of the α_T distribution highlighting the agreement on the sharply falling edge between Data and Monte Carlo for the hadronic selection, in the region $H_T \geq 375$ GeV.

Figure 1.1: Comparisons of 1.1 fb^{-1}2011 7TeV CMS Data and equivalently weighted Monte-Carlo in basic kinematic quantities prior to the α_T selection cut.

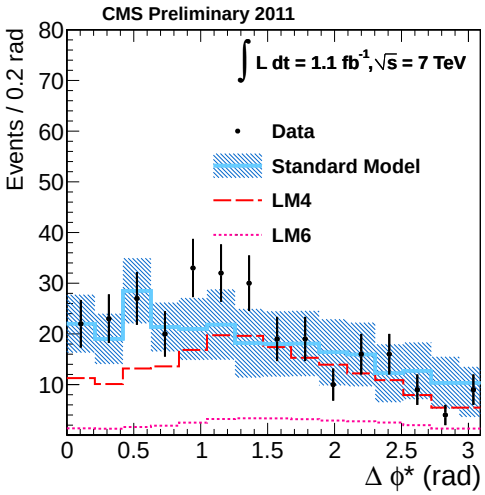

(a) $\Delta\Phi^*$ distribution after α_T selection.

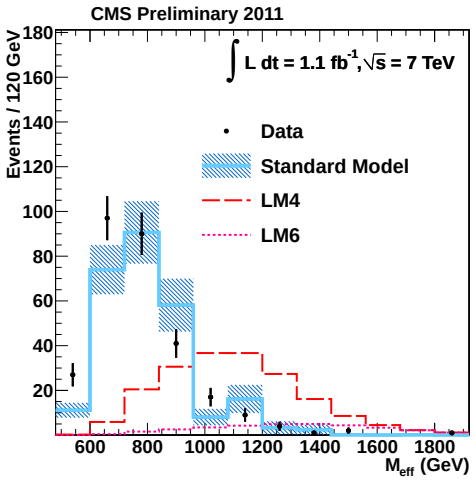

(b) The effective mass distribution, $M_{\text{eff}} = H_T + \text{MHT}$, of the events passing the α_T selection.

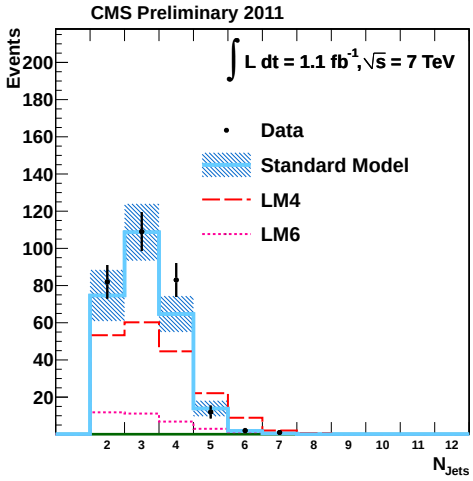

(c) Jet multiplicity after α_T selection.

Figure 1.2: Comparisons of 1.1 fb^{-1}2011 7TeV CMS Data and equivalently weighted Monte-Carlo in basic kinematic quantities after the α_T selection cut.

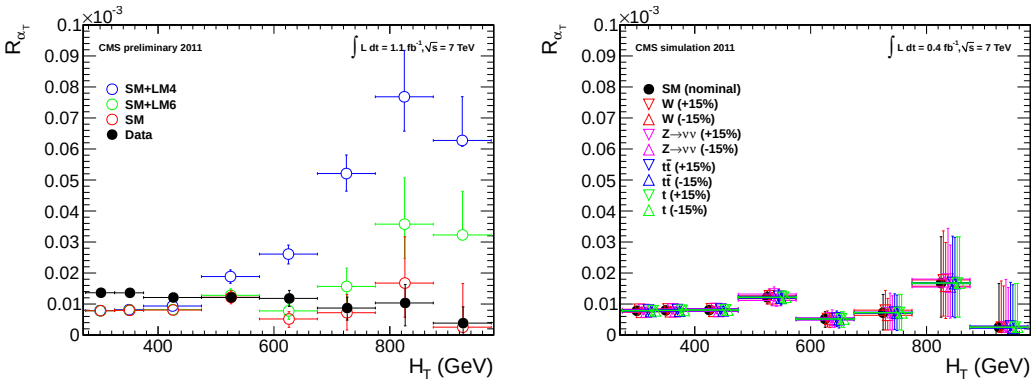

Figure 1.3: (Left) The dependence of R_{α_T} on $H_T$for events with $N_{jet} \geq 2$. (Right) Dependence of rat on $H_T$when varying the effective cross-section of the four major EWK background components individually by $\pm 15\%$. (Markers are artificially offset for clarity.)

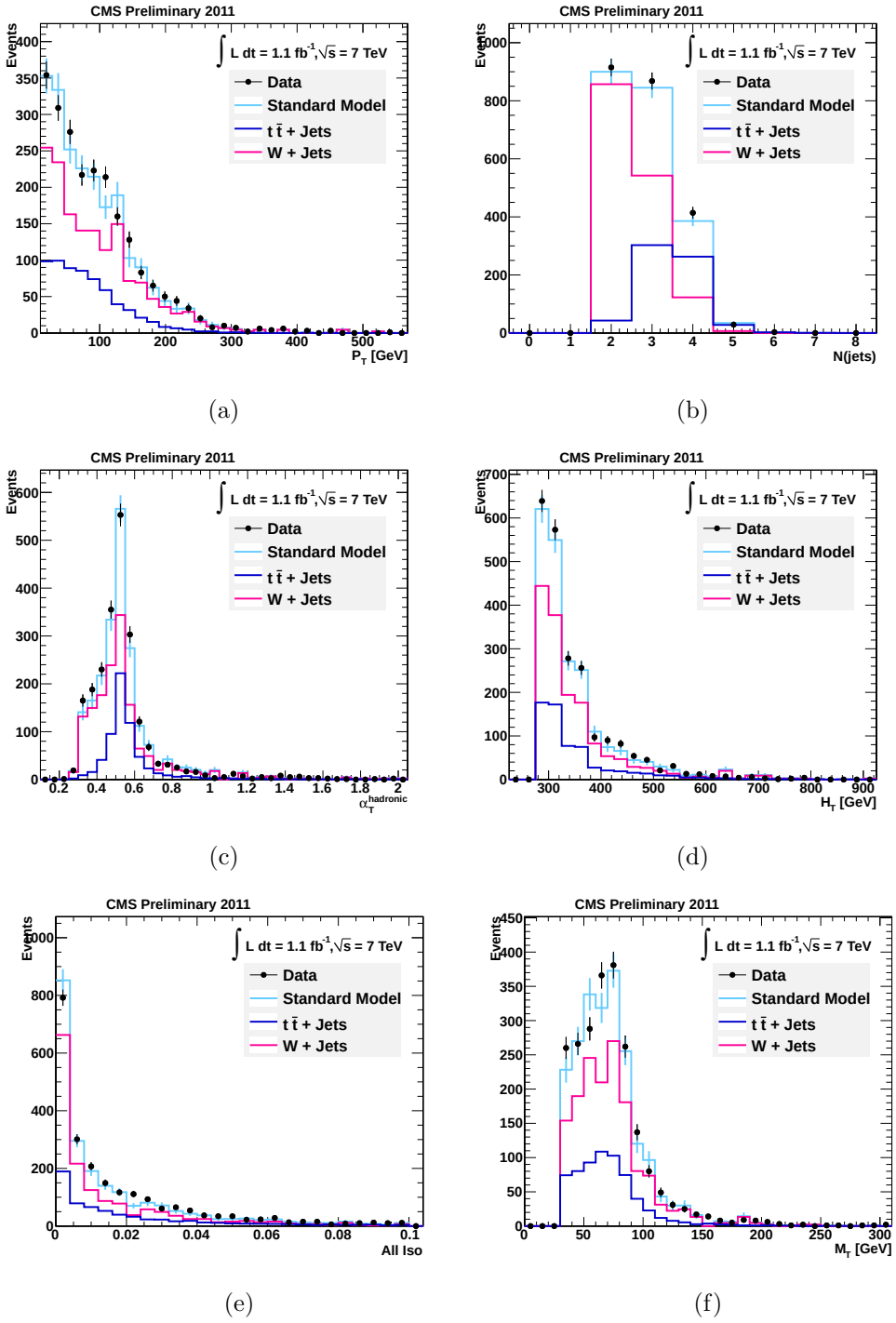

Figure 1.4: Data - Monte Carlo comparisons for the muon control selection before the $\alpha_T > 0.55$ cut is applied, shown for (a) α_T and (b) H_T, (c) Muon Combined Isolation and (d) M_T. A cut of HT >375 GeV has been applied, to select the region of fixed jet thresholds.

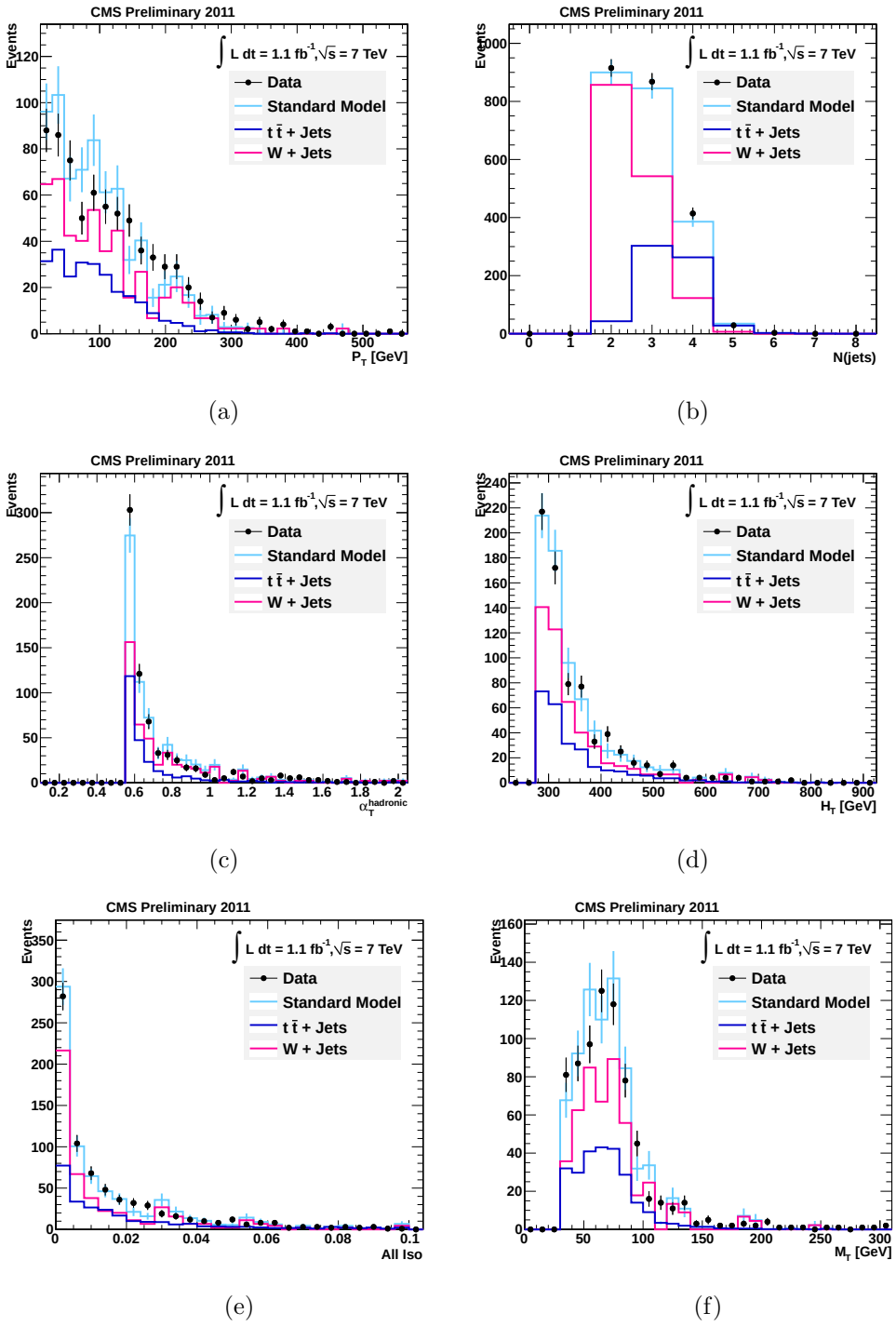

(a) (b)

(c) (d)

(e) (f)

Figure 1.5: Data - Monte Carlo comparisons for the muon control selection after the $\alpha_T > 0.55$ cut is applied, shown for (a) H_{T} and (b) M_T, (c) Muon Combined Isolation and (d) M_T. A cut of HT >375 GeV has been applied, to select the region of fixed jet thresholds.

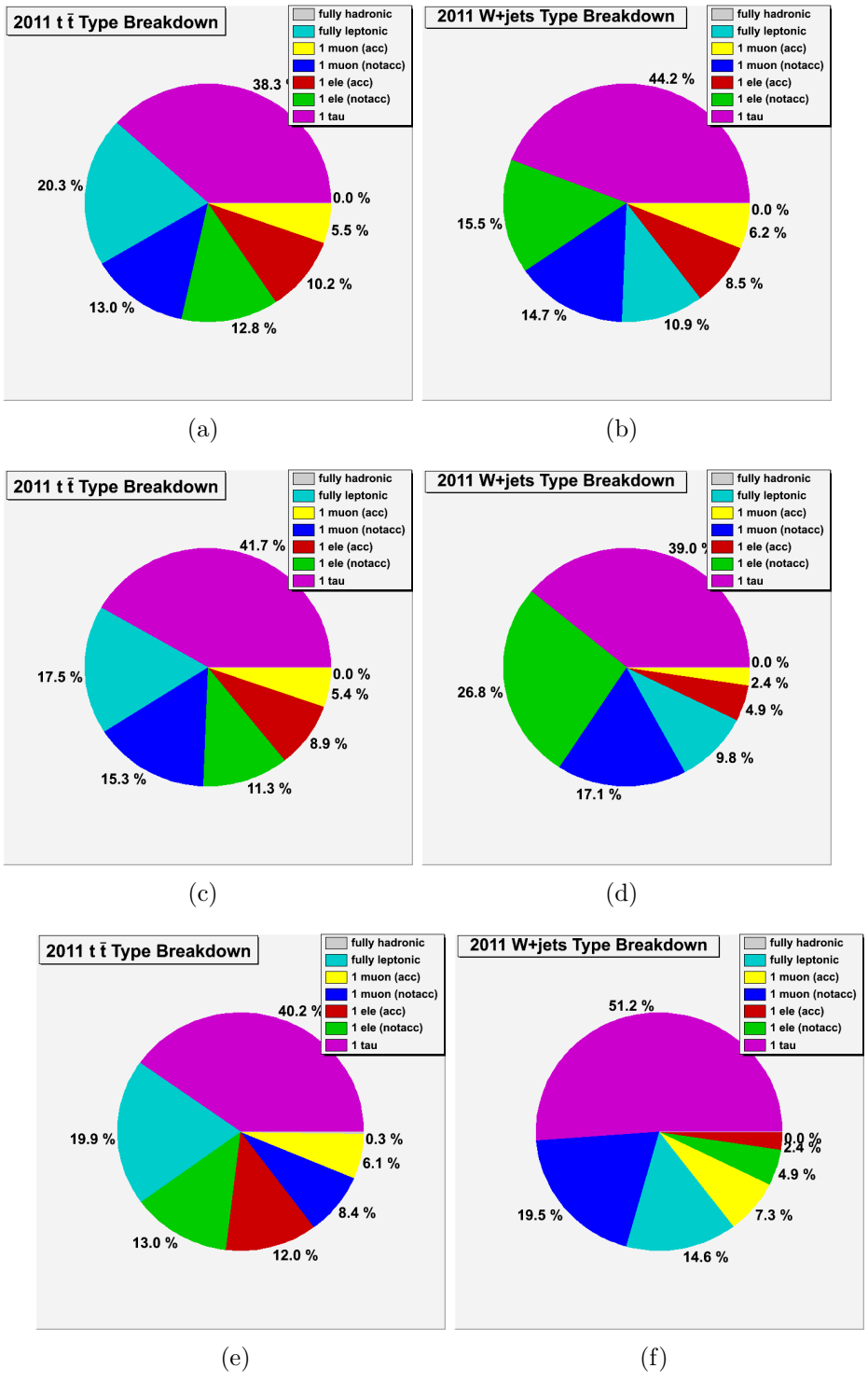

Figure 1.6: Type breakdown of decays resulting in an event selected by the Muon Control selection, shown using Monte-Carlo truth information separately for $t\bar{t}$ + jets (left) and W + jets (right) events. The breakdown is made separately for each jet-scale case: 275 $<H_T<$325 GeV (top), 325 $<H_T<$375 GeV (middle), and $H_T>$375 GeV (bottom).

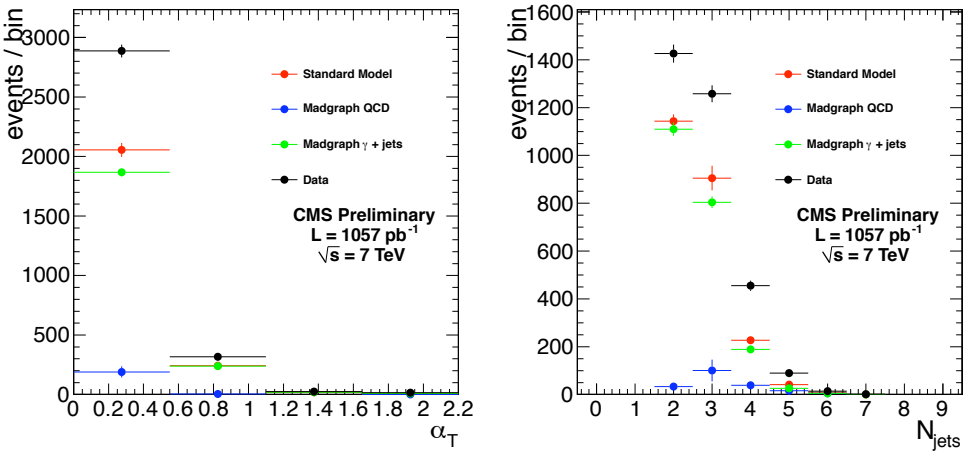

(a) (b)

Figure 1.7: Data-MC comparisons for the photon control sample. $H_{\mathrm{T}} > 375$ GeV and $\not{H}_{\mathrm{T}}/H_{\mathrm{T}} > 0.4$ are required. Left: the distribution of α_T. Right: the distribution of the number of jets.

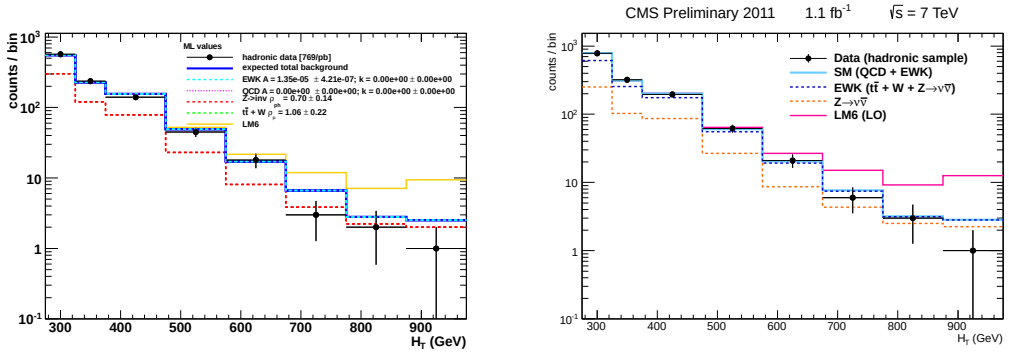

Figure 1.8: H_{T} distribution for events in the hadronic signal sample for scenario a) (left) and scenario b) (right). Shown are the events observed in data (black points), the outcome of the fit (blue line) and a breakdown of the individual background contributions as predicted by the control samples. A possible signal contribution from benchmark point LM6 is indicated as well (yellow line).

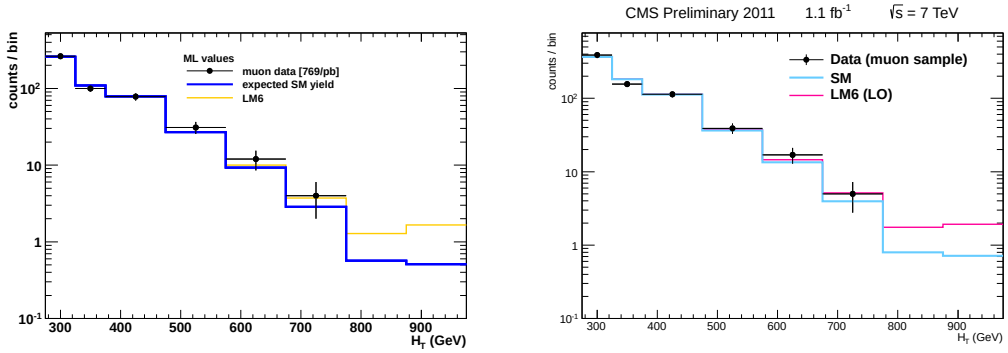

Figure 1.9: H_{T} distribution for events selected in the muon control sample for scenario a) (left) and scenario b) (right). Shown are the events observed in data (black points), the outcome of the fit (blue line) and the MC expectation (dashed line). A possible signal contribution from benchmark point LM6 is indicated as well (yellow line).

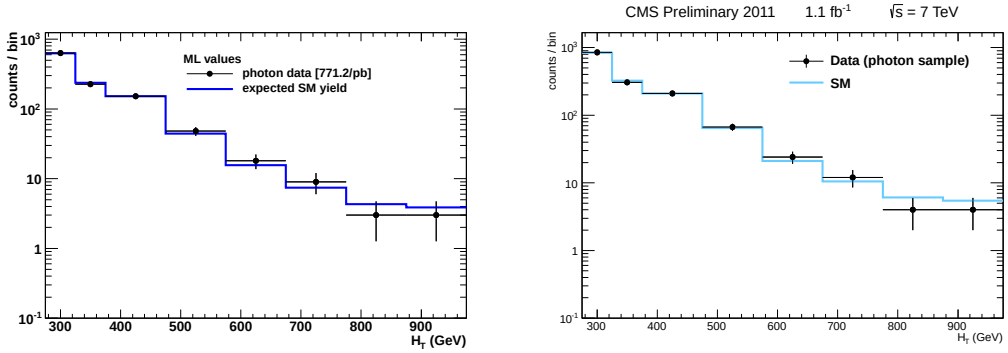

Figure 1.10: H_{T} distribution for events selected in the photon control sample for scenario a) (left) and scenario b) (right). Shown are the events observed in data (black points), the outcome of the fit (blue line) and the MC expectation (dashed line).

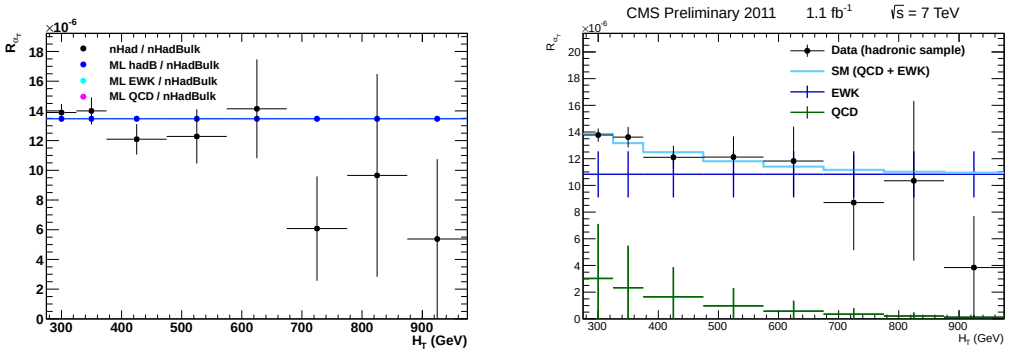

Figure 1.11: R_{α_T} as a function of H_T as observed in data (black points) and the results of the fit assuming different scenarios: a) (left) and b) (right) .

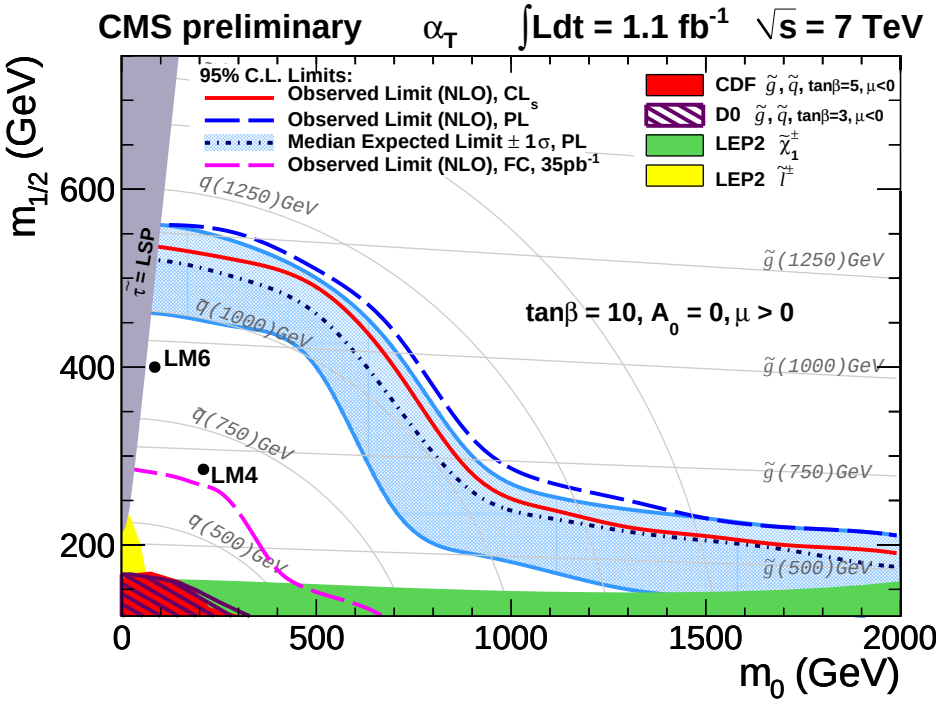

Figure 1.12: Observed and expected 95% CL exclusion contours in the CMSSM $(m_0, m_{1/2})$ plane $(\tan\beta = 10, A_0 = 0, \mu > 0)$ using NLO signal cross sections using the Profile Likelihood (PL) method. The expected limit is shown with its 68% CL range. The observed limit using the CL_s method is shown as well.

Bibliography

[1] Oliver Sim Brning, Paul Collier, P Lebrun, Stephen Myers, Ranko Ostojic, John Poole, and Paul Proudlock. *LHC Design Report*. CERN, Geneva, 2004.

[2] Thomas Sven Pettersson and P Lefvre. The Large Hadron Collider: Conceptual Design. Technical Report CERN-AC-95-05 LHC, CERN, Geneva, Oct 1995.

[3] The CMS Collaboration. The Compact Muon Solenoid Technical Proposal. *CERN/LHCC*, 94-38, 1994.

[4] K et al. Nakamura. Review of particle physics, 2010-2011. review of particle properties. *J. Phys. G*, 37(7A):075021, 2010. The 2010 edition of Review of Particle Physics is published for the Particle Data Group by IOP Publishing as article number 075021 in volume 37 of Journal of Physics G: Nuclear and Particle Physics. This edition should be cited as: K Nakamura et al (Particle Data Group) 2010 J. Phys. G: Nucl. Part. Phys. 37 075021.

[5] The CMS Collaboration. *The CMS hadron calorimeter project: Technical Design Report*. Technical Design Report CMS. CERN, Geneva, 1997.

[6] Efe Yazgan. The CMS barrel calorimeter response to particle beams from 2-GeV/c to 350-GeV/c. *J. Phys. Conf. Ser.*, 160:012056, 2009.

[7] The CMS Collaboration. *The CMS muon project: Technical Design Report*. Technical Design Report CMS. CERN, Geneva, 1997.

[8] Sergio Cittolin, Attila Rcz, and Paris Sphicas. *CMS trigger and data-acquisition project: Technical Design Report*. Technical Design Report CMS. CERN, Geneva, 2002.